Electronic Supplementary Information (ESI)

Fast proton transport enables magnetic relaxation response of graphene quantum dots for monitoring oxidative environment *in vivo*

Yongqiang Li,[a,‡] Hang Wang,[a,b,‡] Caichao Ye,[c] Xuelian Wang,[d] Peng He,[a,b] Siwei Yang,[a,b,*] Hui Dong,[a,b,*] and Guqiao Ding[a,b,*]

[a.] *State Key Laboratory of Materials for Integrated Circuits, Shanghai Institute of Microsystem and Information Technology (SIMIT), Chinese Academy of Sciences (CAS), Shanghai 200050, People's Republic of China. E-mails: yangsiwei@mail.sim.ac.cn; donghui@mail.sim.ac.cn; gqding@mail.sim.ac.cn*
[b.] *Center of Materials Science and Optoelectronics Engineering, University of Chinese Academy of Sciences (UCAS), Beijing 100049, People's Republic of China.*
[c.] *Academy for Advanced Interdisciplinary Studies & Department of Materials Science and Engineering, Guangdong Provincial Key Laboratory of Computational Science and Material Design, Southern University of Science and Technology, Shenzhen, Guangdong 518055, People's Republic of China.*
[d.] *Department of Cardiology, Ruijin Hospital, Shanghai Jiaotong University School of Medicine, Shanghai 200025, People's Republic of China.*
[‡] *These authors contributed equally to this work.*

Supplementary experimental section

Materials

L-cysteine hydrochloride, diethylene glycol (PEG_2, 99.5%), triethylene glycol (PEG_3, 99.0%), tetraethylene glycol (PEG_4, 99.0%), pentaethylene glycol (PEG_5, 98.0%), hexaethylene glycol (PEG_6, 97.0%), heptaethylene glycol (PEG_7, 95%), octaethylene glycol (PEG_8, 98.0%), and gadolinium trinitrate (98%) were purchased from Aladdin Co., Ltd. (Shanghai, China) and used without further purification. Alumina inorganic membrane (220 nm) and dialysis bags (3500 Da) were purchased from CASYUEDA Materials Technology Co., Ltd. (Shanghai, China). Deionized (DI) water (resistivity ~18.2 MΩ cm at 25 °C) was obtained using a Milli-Q system and used throughout all the experiments.

Apparatus

The transmission electron microscopy (TEM) images were captured using JEM-ARM300F (JEOL Ltd.) with a voltage of 80 kV. The X-ray photoelectron spectra (XPS) were obtained using Escalab 250Xi (Thermo Fisher Scientific Inc.). An inductively coupled plasma-optical emission spectrometer (ICP-OES, ICPOES730, Agilent Technologies, Inc.) was used to quantify the Gd^{3+} concentrations. Atomic force microscopy (AFM) experiments were carried out using a Bruker Dimension Icon system. Photoluminescence emission and excitation spectra were recorded in aqueous solution using a PerkinElmer LS55 luminescence spectrometer (PerkinElmer Instruments, U.K.) at room temperature (25 °C). The lifetimes were measured in aqueous solution using Edinburgh FLS1000 (excitation source: picosecond pulsed light emitting diode with wavelength of 320 nm) at room temperature (25 °C).

***In vivo* MRI**

The *in vivo* magnetic resonance imaging (MRI) of the rat was conducted using a Bruker Clinscan 7.0 T MRI scanner with the following parameters:
Echo time = 3 ms, Repetition time = 1000 ms, Number of phase encoding steps = 90, Number of averages = 2, Field of View = 70 mm × 70 mm, Slice thickness = 1.2 mm, Images in acquisition = 25, Spacing between slices = 1.5 mm.
The rat was anesthetized by isoflurane and then laid face down on the sample plane before the scanning. All animal experiments were conducted in accordance with protocols approved by the Ethics Committee of Ruijin Hospital affiliated to Shanghai Jiao Tong University School of Medicine.

Supplementary figures

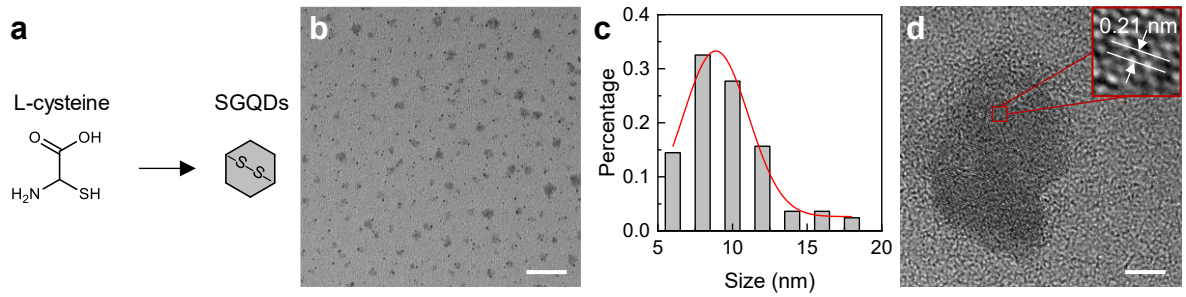

Fig. S1 Morphological characterizations of SGQDs. (a) Synthesis of SGQDs using hydrothermal treatment. The regular hexagons fill in grey represent the SGQDs. 100 mg of L-cysteine hydrochloride is dissolved in 100 mL of DI water for hydrothermal reaction (150 ^{o}C, 12 h). (b) The TEM image of SGQDs. Scale bar: 100 nm. (c) The size distribution histogram acquired from Fig. S1a. The *Sturges*' method was used to plot the particle size histogram by counting 83 particles. A Gaussian distribution was used to obtain the average size of SGQDs (8.89 nm). (d) The high-resolution TEM of SGQDs. Scale bar: 5 nm. Inset: the lattice spacing of SGQDs is 0.21 nm, corresponding to the [1120] lattice fringes of graphene.

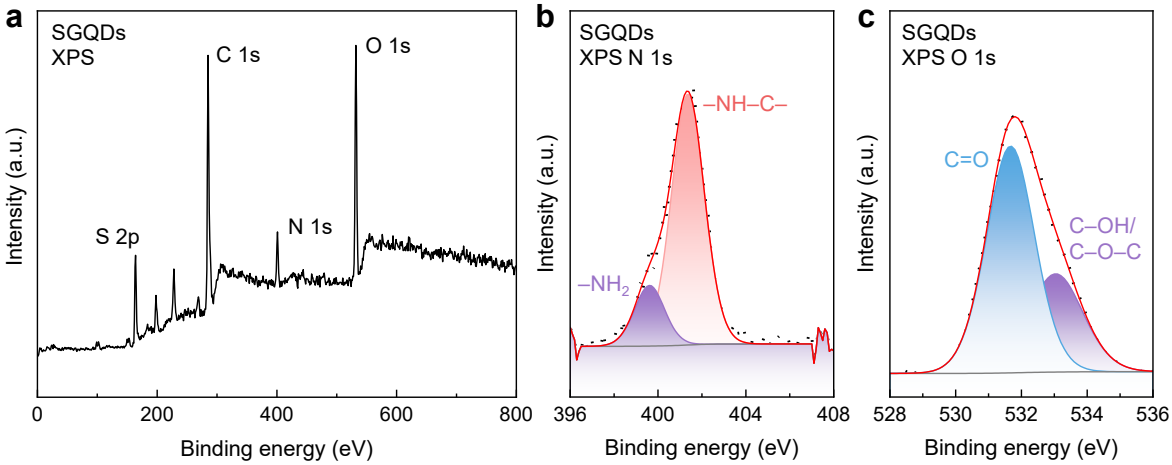

Fig. S2 Structure characterizations of SGQDs. (a) The XPS spectrum of SGQDs. Peaks located at 284.91, 401.32, 531.87, and 163.61 eV can be recognized as the C 1s, N 1s, O 1s, and S 2p signals of SGQDs, respectively. The atomic contents of C, N, O, and S in SGQDs are 60.96, 8.09, 21.13, and 9.82 at.%, respectively. Data acquired from the combustion elemental analyzer also confirms the contents of C, N, O, and S are 56.31, 9.53, 20.34, and 13.82 at.%, which are equivalent to the XPS results. (b) The XPS N 1s spectrum of SGQDs. The two peaks around 399.64 and 401.38 eV can be recognized as $-NH_2$ and –NH–C– bonds, respectively. (c) The XPS O 1s spectrum of SGQDs. peaks at 531.67 and 533.04 eV contribute to the C=O and C−OH/C−O−C bonds, respectively.

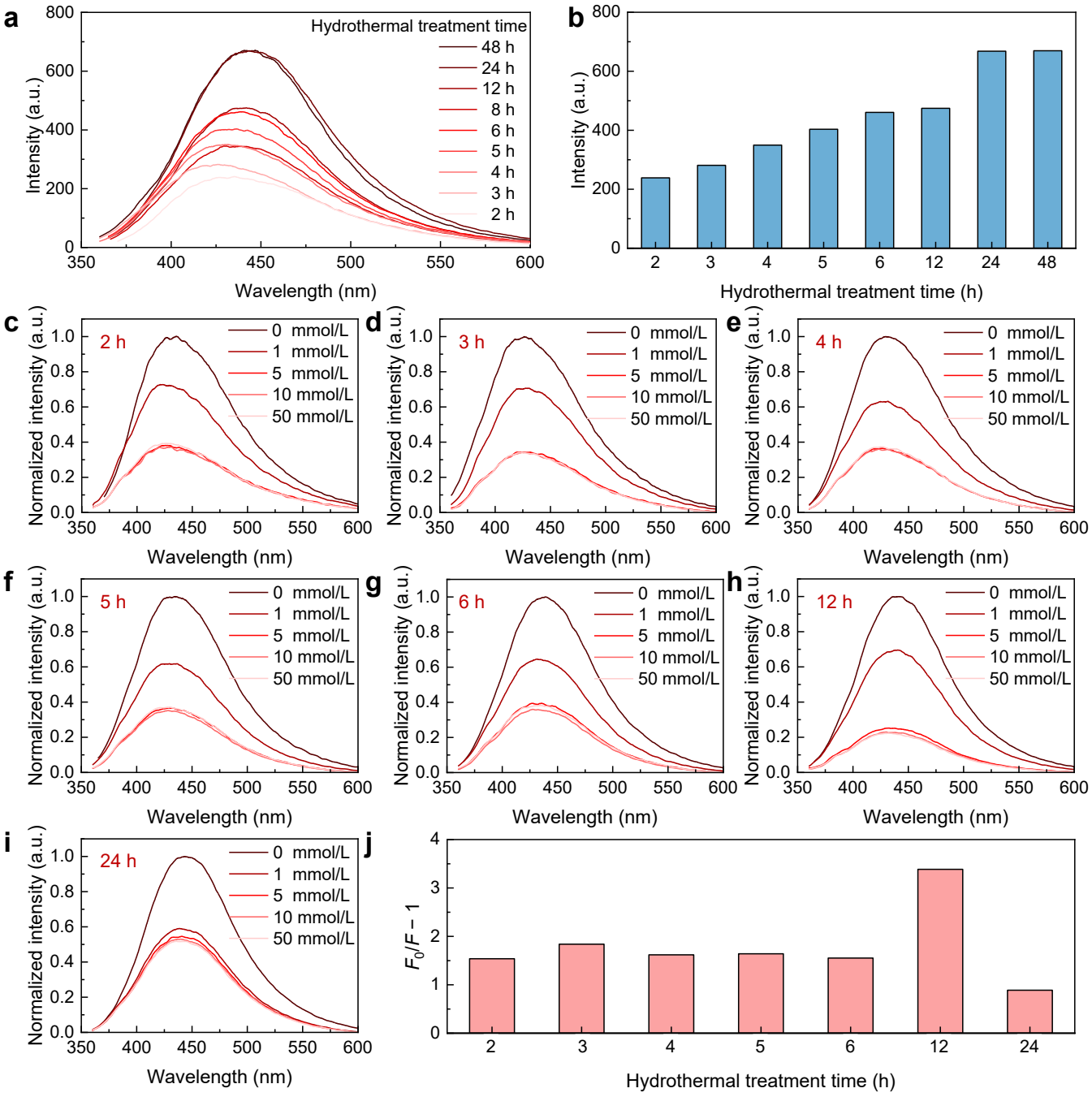

Fig. S3 Optimization of hydrothermal treatment time for synthesizing SGQDs. (a) The fluorescence emission spectra and (b) comparison of fluorescent intensity of SGQDs synthesized with different hydrothermal treatment times. The fluorescent emission intensity increases with the increasing hydrothermal treatment time. (c)–(i) The fluorescence emission spectra (data was smoothed, normalized fluorescent intensities) of SGQDs after reacting with H_2O_2 with different concentrations for 12 h. 0 mmol/L of H_2O_2 represents the blank test. The SGQDs used are synthesized by the hydrothermal treatment for (c) 2 h, (d) 3 h, (e) 4 h, (f) 5 h, (g) 6 h, (h) 12 h, and (i) 24 h. (j) Comparison of the fluorescent intensity change of SGQDs synthesized with different hydrothermal treatment times. F_0 and F represent the fluorescent intensities of SGQDs before and after the reaction with H_2O_2 (50 mmol/L), respectively. The SGQDs synthesized *via* hydrothermal treatment for 12 h show the largest change after reaction with H_2O_2, the SGQDs (12 h) are therefore used in the following experiments.

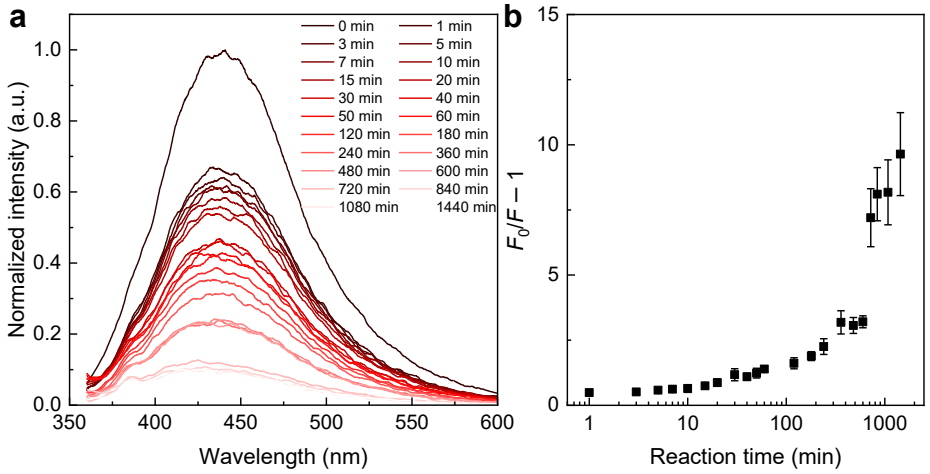

Fig. S4 Optimization of reaction between SGQDs and H_2O_2. (a) The fluorescence emission spectra and (b) comparison of fluorescent intensity of SGQDs after the reaction with H_2O_2 (50 mmol/L) for different times. F_0 and F represent the fluorescent intensities of SGQDs before and after the reaction with H_2O_2, respectively. The fluorescent intensity of SGQDs is reduced as the reaction time increases.

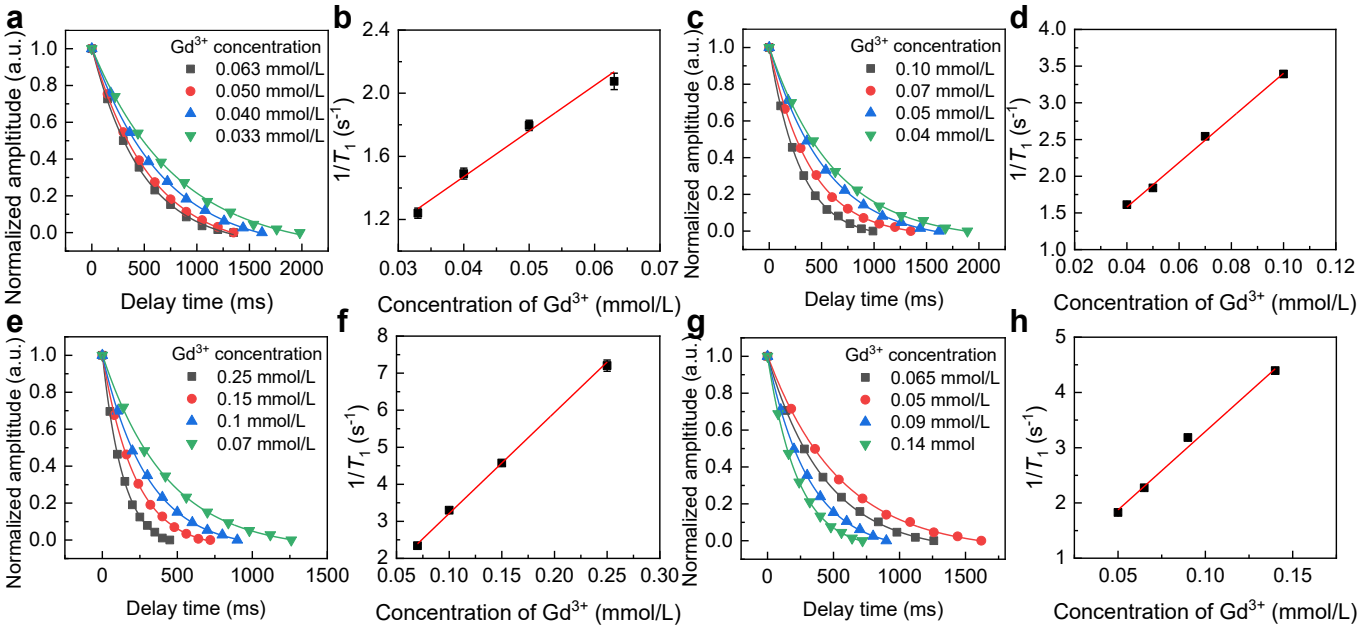

Fig. S5 Optimization of the ratio of L-cysteine hydrochloride to Gd^{3+} for synthesizing SGQDS-Gd. The (a) T_1 fittings and (b) longitudinal relaxivity (r_1) fittings of SGQDs-Gd. 100 mg of L-cysteine hydrochloride and 0.5 mmol/L of Gd^{3+} were dissolved in 100 mL of DI water for hydrothermal reaction (150 °C, 12 h) to obtain the SGQDs-Gd. The T_1 values of SGQDs-Gd aqueous solution are 481.87 ± 13.00, 556.63 ± 10.99, 670.78 ± 16.82, and 806.33 ± 22.85 ms when the Gd^{3+} concentrations are 0.063, 0.05, 0.04, and 0.03 mmol/L with the adjusted R^2 values of 0.99934, 0.99971, 0.99953, and 0.99938, respectively. The r_1 of SGQDs-Gd aqueous solution is fitted as 28.92 ± 2.50 L $mmol^{-1}$ s^{-1} with an adjusted R^2 of 0.97789. The (c) T_1 fittings and (d) r_1 fittings of SGQDs-Gd. 100 mg of L-cysteine hydrochloride and 1 mmol/L of Gd^{3+} were dissolved in 100 mL of DI water for hydrothermal reaction (150 °C, 12 h) to obtain the SGQDs-Gd. The T_1 values of SGQDs-Gd aqueous solution are 294.77 ± 4.19, 393.18 ± 6.60, 543.50 ± 7.42, 620.38 ± 11.96 ms when the Gd^{3+} concentrations are 0.10, 0.07, 0.05, and 0.04 mmol/L with the adjusted R^2 values of 0.99977, 0.99968, 0.99979, and 0.99962, respectively. The r_1 of SGQDs-Gd aqueous solution is fitted as 30.41 ± 1.44 L $mmol^{-1}$ s^{-1} with an adjusted R^2 of 0.99330. The (e) T_1 fittings and (f) r_1 fittings of SGQDs-Gd. 100 mg of L-cysteine hydrochloride and 5 mmol/L of Gd^{3+} were dissolved in 100 mL of DI water for hydrothermal reaction (150 °C, 12 h) to obtain the SGQDs-Gd. The T_1 values of SGQDs-Gd aqueous solution are 138.83 ± 3.94, 218.64 ± 3.31, 303.12 ± 5.7, and 427.17 ± 9.71 ms when the Gd^{3+} concentrations are 0.25, 0.15, 0.10, and 0.01 mmol/L with the adjusted R^2 values of 0.99944, 0.99975, 0.99965, and 0.99950, respectively. The r_1 of SGQDs-Gd aqueous solution is fitted as 27.26 ± 1.01 L $mmol^{-1}$ s^{-1} with an adjusted R^2 of 0.99592. The (g) T_1 fittings and (h) r_1 fittings of SGQDs-Gd. 100 mg of L-cysteine hydrochloride and 10 mmol/L of Gd^{3+} were dissolved in 100 mL of DI water for hydrothermal reaction (150 °C, 12 h) to obtain the SGQDs-Gd. The T_1 values of SGQDs-Gd aqueous solution are 227.52 ± 1.67, 314.17 ± 4.61, 439.63 ± 6.51, and 547.48 ± 12.78 ms when the Gd^{3+} concentrations are 0.14, 0.09, 0.065, and 0.05 mmol/L with the adjusted R^2 values of 0.99947, 0.99979, 0.99980, and 0.99994, respectively. The r_1 of SGQDs-Gd aqueous solution is fitted as 28.38 ± 1.48 L $mmol^{-1}$ s^{-1} with an adjusted R^2 of 0.99192. Based on the above results, the optimal ratio of L-cysteine hydrochloride to Gd^{3+} for synthesizing SGQDS-Gd is 100 mg to 1 mmol/L when dissolved in 100 mL of DI water.

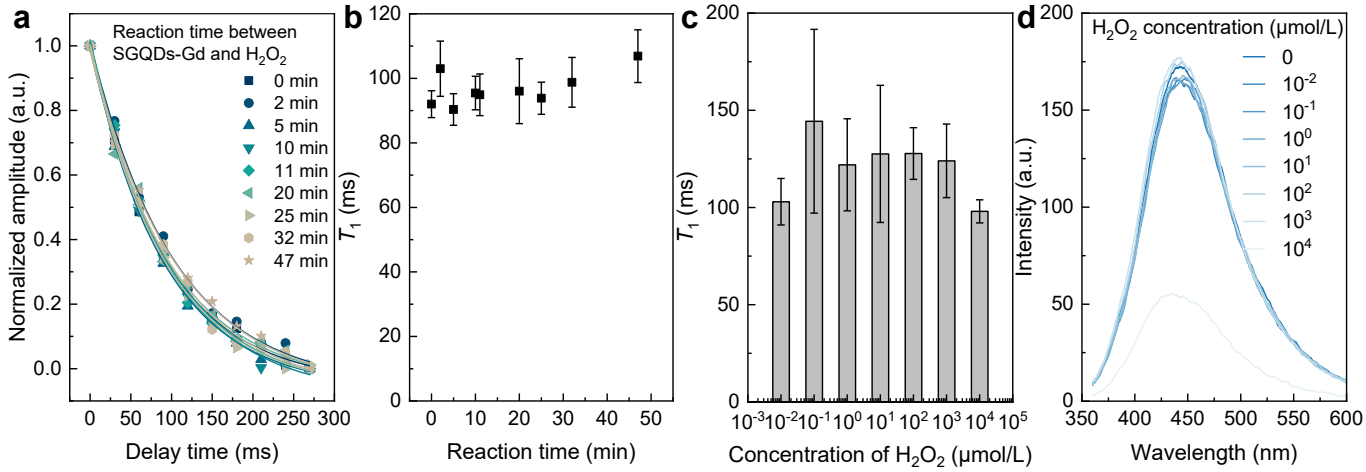

Fig. S6 Detection of H_2O_2 using SGQDs-Gd (0.2 mmol/L). (a) T_1 fittings of SGQDs-Gd before and after reaction with H_2O_2 (50 mmol/L) for different times. T_1 values SGQDs-Gd aqueous solution are 92.01 ± 4.50, and 102.98 ± 9.26, 90.36 ± 5.28, 95.45 ± 5.62, 94.90 ± 6.96, 96.02 ± 10.86, 93.83 ± 5.39, 98.78 ± 8.33, and 106.88 ± 8.82 ms when the reaction times between SGQDs-Gd and H_2O_2 are 0, 2, 5, 10, 11, 20, 25, 32, and 47 min, respectively. A scatter diagram in (b) reveals the T_1 of SGQDs-Gd has no significant change when reacting with H_2O_2. Error bars indicate the error of fitting. (c) The T_1 values of SGQDs-Gd when reacting with H_2O_2 (different concentrations) after 12 h. When the H_2O_2 concentration is 0 (blank), the T_1 of SGQDs-Gd is 117.37 ± 21.42 ms. When increasing the H_2O_2 concentration, the T_1 doesn't show significant change compared to that of the blank sample. Error bars indicate the standard deviation (SD) of three replicates of the test. (d) The fluorescence emission spectra of SGQDs-Gd after reacting with H_2O_2 for 12 h. The fluorescent intensity of SGQDs-Gd shows a significant reduction after reacting with H_2O_2 (10 mmol/L) for 12 h, indicating the SGQDs in SGQDs-Gd still have the ability to sense H_2O_2 after connecting with Gd^{3+}.

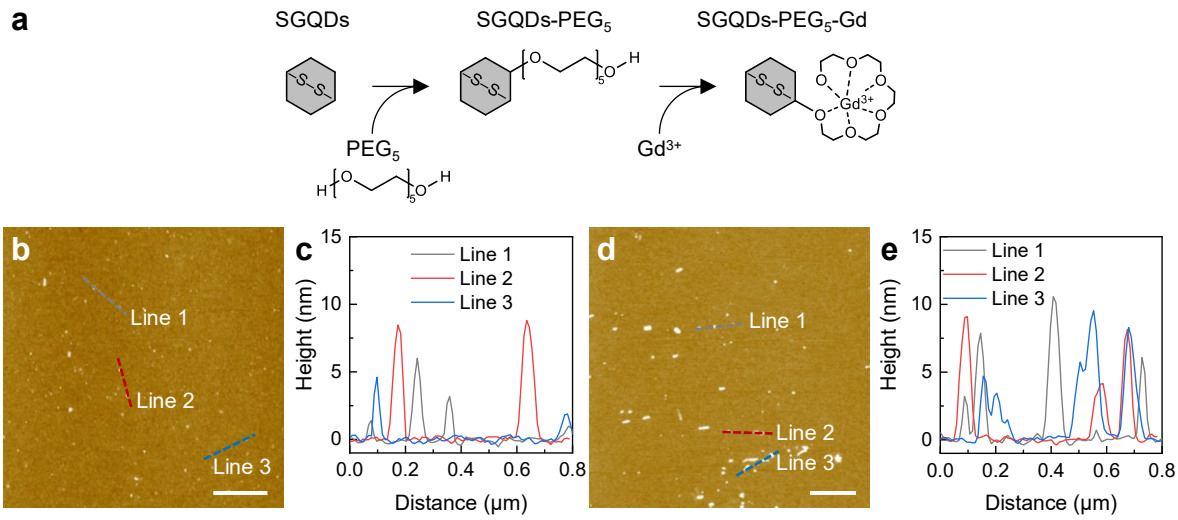

Fig. S7 Synthesis of SGQDs-PEG_5-Gd and the AFM characterizations. (a) Hydrothermal treatment for synthesizing SGQDs-PEG_5-Gd. 0.1 mmol of PEG_5 was added into the prepared SGQDs (100 mL) and heated at 150 °C for 6 h. Next, 0.1 mmol Gd^{3+} was added to the mixture and heated at 150 °C for another 6 h. PEG_5 can be replaced with other PEG chains for synthesizing SGQDs-PEG_n-Gd. The purification of SGQDs-PEG_n-Gd is the same as the purification of SGQDs. (b) The AFM image of SGQDs-PEG_5 distributed on a SiO_2/Si substrate. Scale bar: 1 μm. (c) The height profiles of lines 1–3 marked in (b). The measured thickness of SGQDs-PEG_5 ranges from 2 to 9 nm, revealing that most SGQDs-PEG_5 nanoparticles contain 6 to 27 layers. (d) The AFM image of SGQDs-PEG_5-Gd distributed on a SiO_2/Si substrate. Scale bar: 1 μm. (e) The height profiles of lines 1–3 marked in (d). The measured thickness of SGQDs-PEG_5-Gd ranges from 3 to 9 nm, revealing that most SGQDs-PEG_5-Gd nanoparticles contain 10 to 27 layers. The SGQDs thicken after the modification of PEG_5 but keep the thickness after the binding of Gd^{3+}.

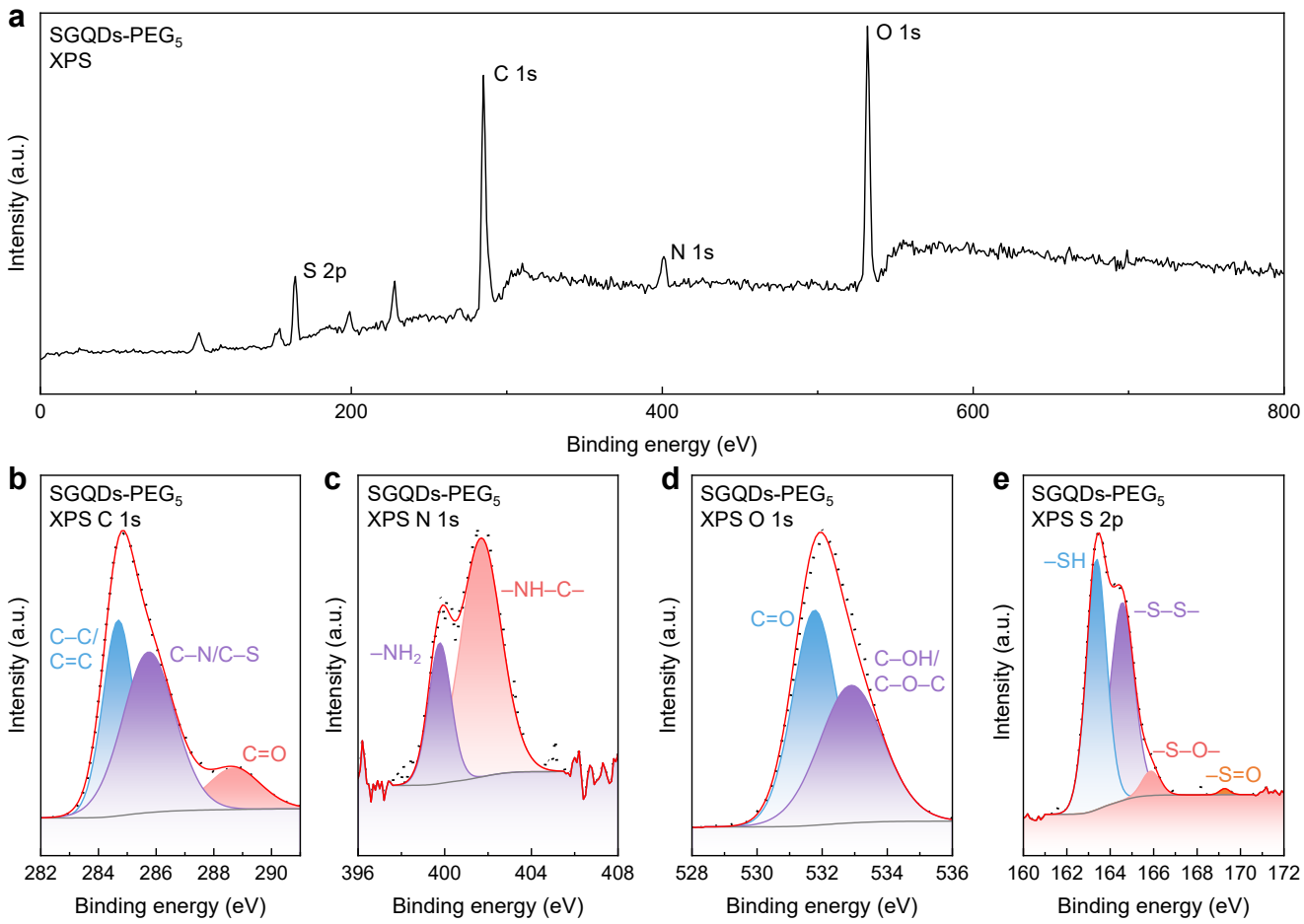

Fig. S8 Structure characterizations of SGQDs-PEG_5. (a) The XPS spectrum of SGQDs-PEG_5. Peaks located at 284.94, 401.63, 532.09, and 163.63 eV can be recognized as the C 1s, N 1s, O 1s, and S 2p signals of SGQDs-PEG_5, respectively. The atomic contents of C, N, O, and S in SGQDs-PEG_5 are 63.31, 5.99, 22.91, and 7.79 at.%, respectively. The increased proportions of C and O compared to those of SGQDs (Fig. S2a) indicate the introduction of PEG_5 in the structure. (b) XPS C 1s spectrum of SGQDs-PEG_5. Peaks located at 284.69, 285.75, and 288.68 eV can be regarded as the C–C/C=C, C–N/C–S, and C=O bonds, respectively. (c) The XPS N 1s spectrum of SGQDs-PEG_5. The two peaks around 399.76 and 401.69 eV can be recognized as $-NH_2$ and –NH–C– bonds, respectively. (d) XPS O 1s spectrum of SGQDs-PEG_5. Peaks at 531.82 and 532.95 eV can be recognized as C=O and C–OH/C–O–C bonds, respectively. (e) XPS S 2p spectrum of SGQDs-PEG_5. Peaks at 163.37, 164.53, 165.87, and 169.27 eV can be regarded as the –SH, –S–S–, –S–O–, and –S=O bonds, respectively.

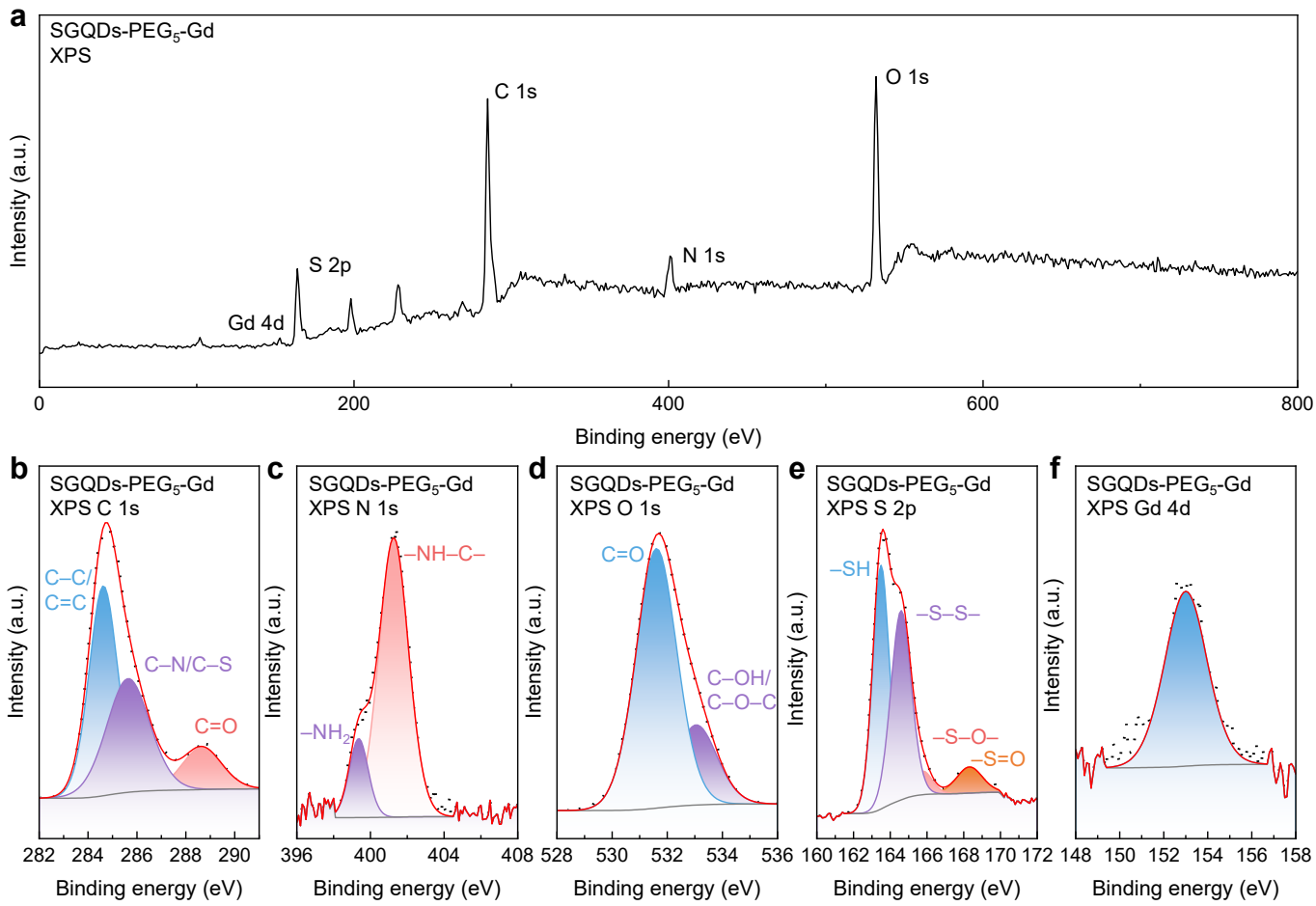

Fig. S9 Structure characterizations of SGQDs-PEG$_5$-Gd. (a) The XPS spectrum of SGQDs-PEG$_5$-Gd. Peaks located at 284.79, 401.27, 531.71, 163.79, and 152.91 eV can be recognized as the C 1s, N 1s, O 1s, S 2p, and Gd 4d signals of SGQDs-PEG$_5$-Gd, respectively. The atomic contents of C, N, O, S, and Gd in SGQDs-PEG$_5$-Gd are 58.59, 8.43, 22.22, 10.51, and 0.25 at.%, respectively. (b) XPS C 1s spectrum of SGQDs-PEG$_5$-Gd. Peaks located at 284.71, 285.81, and 288.71 eV can be regarded as the C–C/C=C, C–N/C–S, and C=O bonds, respectively. (c) The XPS N 1s spectrum of SGQDs-PEG$_5$-Gd. The two peaks around 399.43 and 401.38 eV can be recognized as –NH$_2$ and –NH–C– bonds, respectively. (d) XPS O 1s spectrum of SGQDs-PEG$_5$-Gd. Peaks at 531.66 and 533.10 eV can be recognized as C=O and C–OH/C–O–C bonds, respectively. (e) XPS S 2p spectrum of SGQDs-PEG$_5$-Gd. Peaks at 163.36, 164.30, 164.94, and 168.77 eV can be regarded as the –SH, –S–S–, –S–O–, and –S=O bonds, respectively. (f) XPS Gd 4d spectrum of SGQDs-PEG$_5$-Gd.

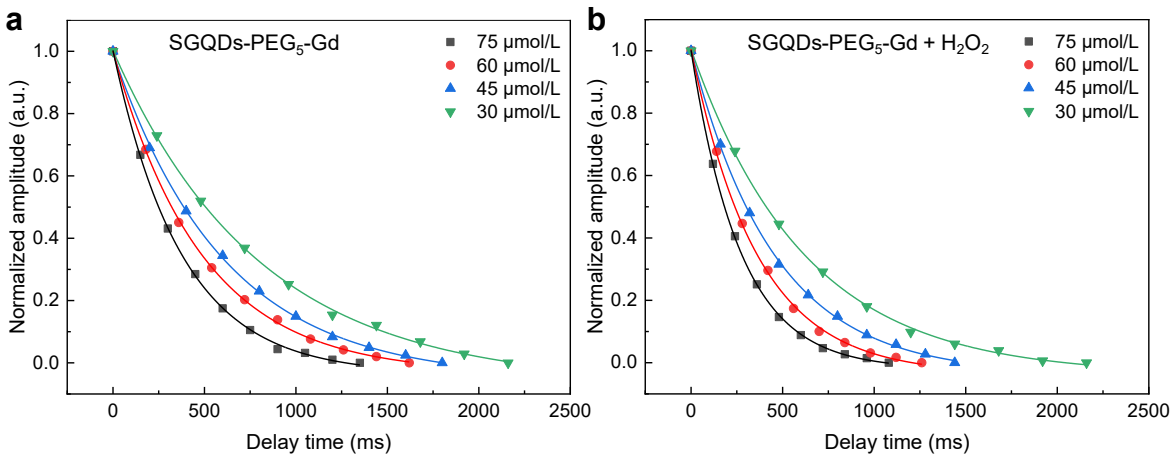

Fig. S10 T_1 fittings of SGQDs-PEG$_5$-Gd. (a) T_1 fittings of SGQDs-PEG$_5$-Gd with different Gd^{3+} concentrations. The T_1 values are 377.22 ± 7.73, 486.23 ± 7.73, 605.36 ± 11.78, and 799.47 ± 21.74 ms when the Gd^{3+} concentrations are 75, 60, 45, and 30 μmol/L with adjusted R^2 values of 0.99950, 0.99972, 0.99963, and 0.99936, respectively. (b) T_1 fittings of SGQDs-PEG$_5$-Gd after reacting with H_2O_2 (10 mmol/L, 12 h) with different Gd^{3+} concentrations. The T_1 values are 270.48 ± 3.11, 360.86 ± 8.32, 456.69 ± 8.37, and 620.67 ± 13.71 ms when the Gd^{3+} concentrations are 75, 60, 45, and 30 μmol/L with adjusted R^2 values of 0.99983, 0.99938, 0.99965, and 0.99943, respectively.

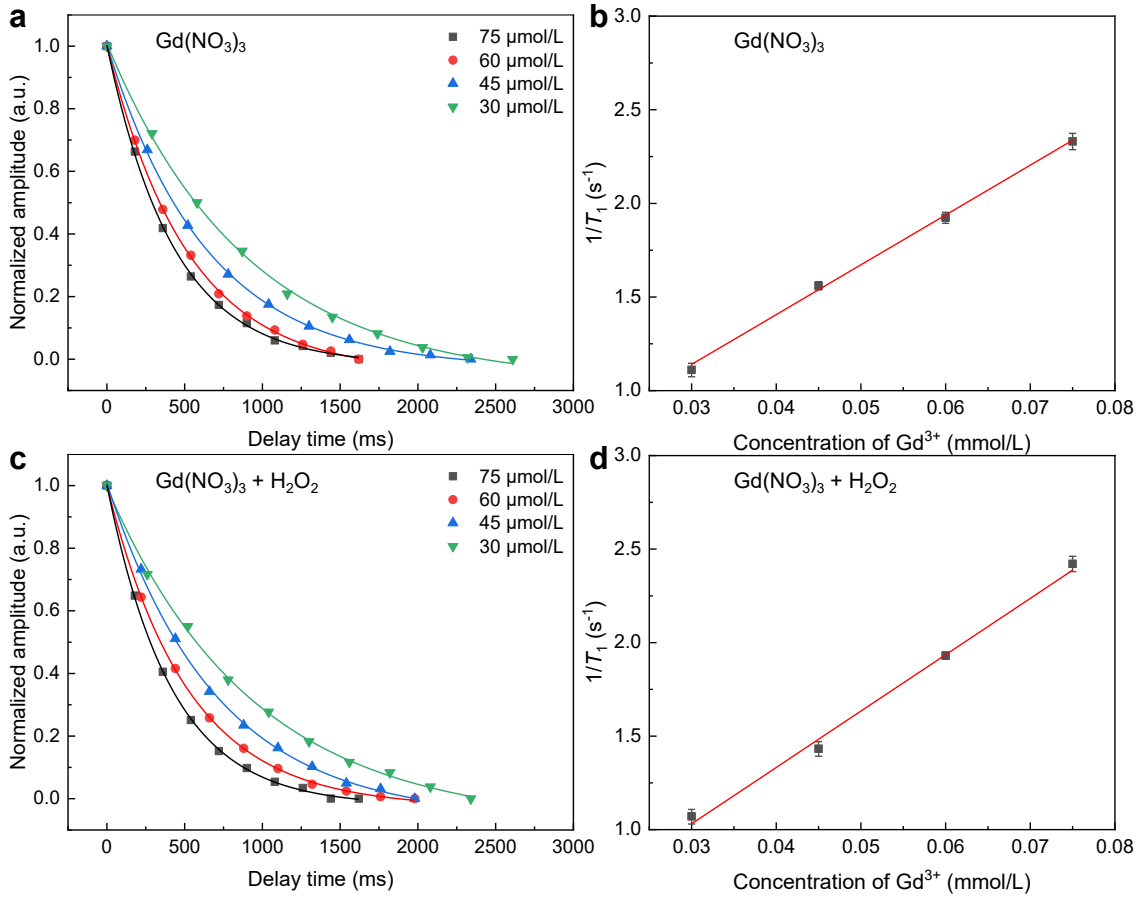

Fig. S11 The T_1 and r_1 fittings of $Gd(NO_3)_3$ aqueous solution. (a) T_1 fittings of $Gd(NO_3)_3$ aqueous solution with different Gd^{3+} concentrations. The T_1 values are 428.91 ± 8.17, 520.15 ± 8.47, 641.13 ± 9.21, and 900.05 ± 29.09 ms when the Gd^{3+} concentrations are 75, 60, 45, and 30 μmol/L with adjusted R^2 values of 0.99954, 0.99973, 0.99975, and 0.99901, respectively. (b) The r_1 fitting of $Gd(NO_3)_3$ aqueous solution. The r_1 is fitted as 26.60 ± 1.07 L $mmol^{-1}$ s^{-1} with an adjusted R^2 of 0.99519. (c) The T_1 fittings of $Gd(NO_3)_3$ aqueous solution with different Gd^{3+} concentrations after reacting with 10 mmol/L of H_2O_2 for 12 h. The T_1 values are 413.61 ± 6.87, 517.72 ± 5.12, 697.84 ± 19.43, and 934.33 ± 34.13 ms when the Gd^{3+} concentrations are 75, 60, 45, and 30 μmol/L with adjusted R^2 values of 0.99964, 0.99988, 0.99928, and 0.99895, respectively. (d) The r_1 fittings of $Gd(NO_3)_3$ aqueous solution after reacting with 10 mmol/L of H_2O_2 for 12 h. The r_1 is fitted as 30.14 ± 1.48 L $mmol^{-1}$ s^{-1} with an adjusted R^2 of 0.99276. The r_1 values of $Gd(NO_3)_3$ aqueous solution before and after the reaction with H_2O_2 show a slight difference.

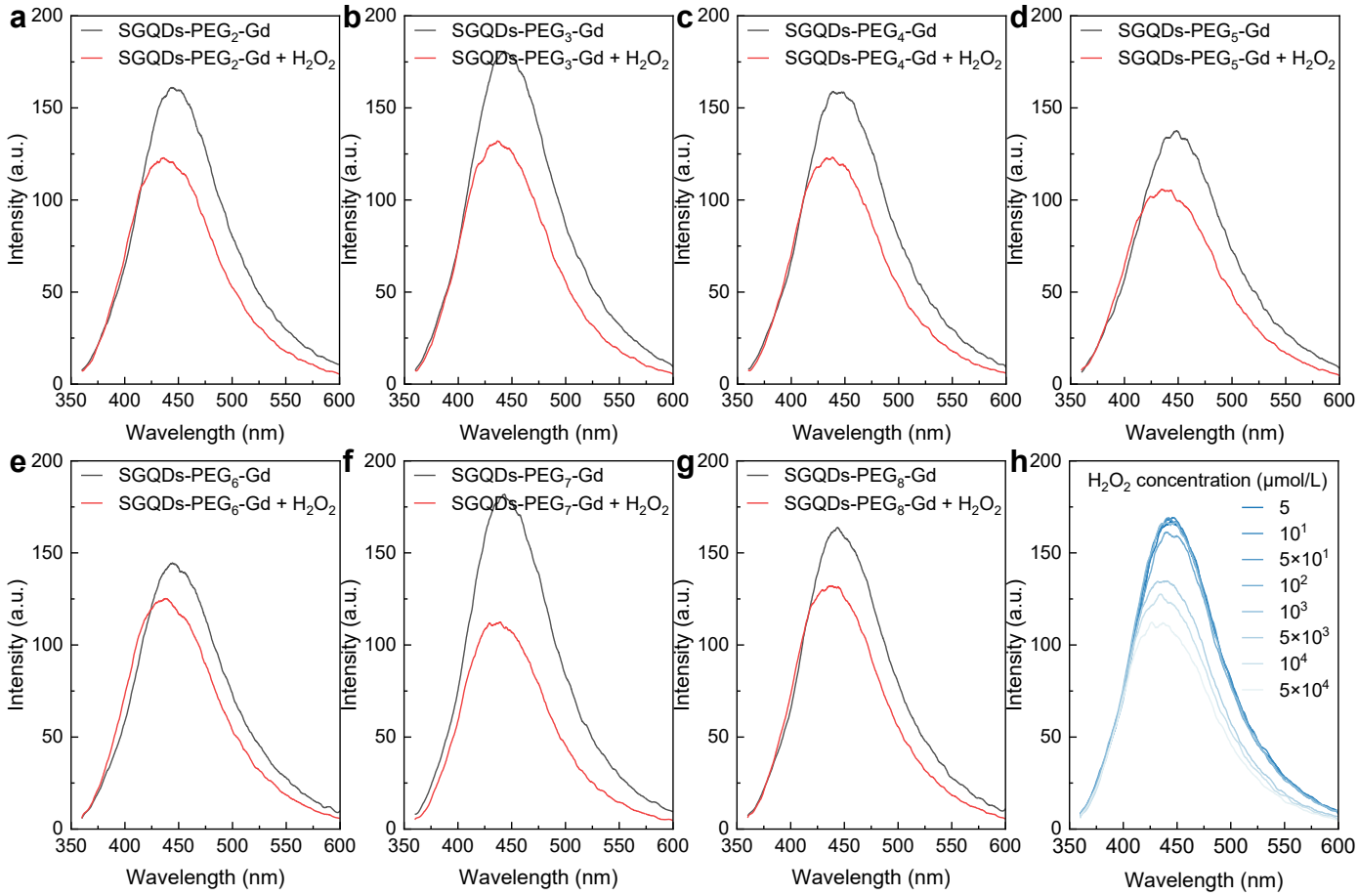

Fig. S12 Fluorescence emission spectra of SGQDs-PEG$_n$-Gd (n = 2–8) before and after reacting with H_2O_2 for 12 h. The fluorescence emission spectra of (a) SGQDs-PEG$_2$-Gd, (b) SGQDs-PEG$_3$-Gd, (c) SGQDs-PEG$_4$-Gd, (d) SGQDs-PEG$_5$-Gd, (e) SGQDs-PEG$_6$-Gd, (f) SGQDs-PEG$_7$-Gd, and (g) SGQDs-PEG$_8$-Gd before and after reacting with H_2O_2 (10 mmol/L) for 12 h. The fluorescent intensities of SGQDs-PEG$_n$-Gd (n = 2–8) show significant reduction after the reaction with H_2O_2. (h) Fluorescence emission spectra of SGQDs-PEG$_5$-Gd after reacting with H_2O_2 (different concentrations) for 12 h. The fluorescent intensity of SGQDs-PEG$_5$-Gd decreases with the increase of H_2O_2 concentration.

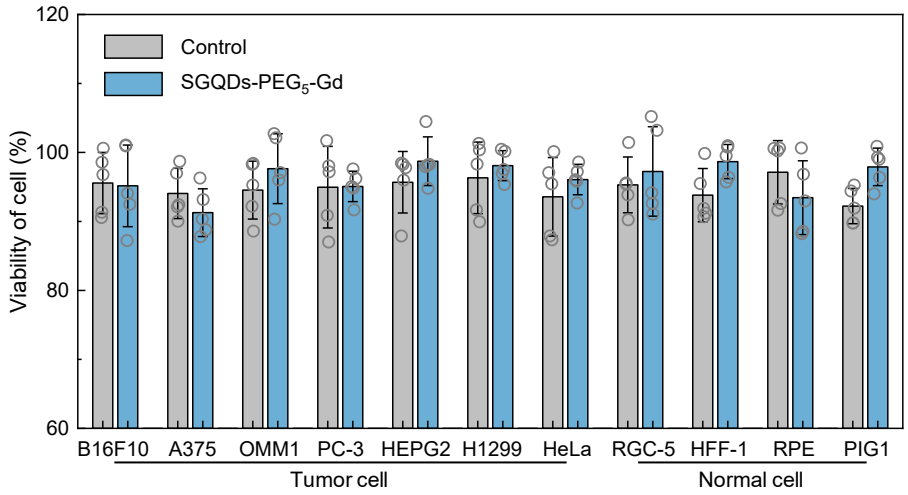

Fig. S13 Viabilities of various tumor and normal cells after incubation with SGQDs-PEG_5-Gd (200 μg/mL) for 48 h. Compared to the control group, cells incubated with SGQDs-PEG_5-Gd show no obvious change in cell survival rate. Error bars indicate the SD of five replicates of the test.